Naval Research Laboratory
Washington, DC 20375-5320

NRL/MR/6410--96-7898

DDG-51 Flt-IIA Airwake Study Part 2: Hangar Interior Flow

ALEXANDRA M. LANDSBERG
WILLIAM C. SANDBERG
THEODORE R. YOUNG, JR.
JAY P. BORIS

Center for Reactive Flow and Dynamical Systems
Laboratory for Computational Physics and Fluid Dynamics

November 15, 1996

REPORT DOCUMENTATION PAGE

Form Approved
OMB No. 0704-0188

1. AGENCY USE ONLY (*Leave Blank*)	2. REPORT DATE	3. REPORT TYPE AND DATES COVERED
	November 15, 1996	

4. TITLE AND SUBTITLE

DDG-51 Flt-IIA Airwake Study Part 2: Hangar Interior Flow

5. FUNDING NUMBERS

PE - 63721N

6. AUTHOR(S)

A.M. Landsberg, W.C. Sandberg, T.R. Young, Jr., and J.P. Boris

7. PERFORMING ORGANIZATION NAME(S) AND ADDRESS(ES)

Naval Research Laboratory
Washington, DC 20375-5320

8. PERFORMING ORGANIZATION REPORT NUMBER

NRL/MR/6410--96-7898

9. SPONSORING/MONITORING AGENCY NAME(S) AND ADDRESS(ES)

Naval Sea Systems Command
Code 03DB, 2531 Jefferson Davis Highway
Arlington, VA 22242-5160

10. SPONSORING/MONITORING AGENCY REPORT NUMBER

11. SUPPLEMENTARY NOTES

12a. DISTRIBUTION/AVAILABILITY STATEMENT

Approved for public release; distribution unlimited.

12b. DISTRIBUTION CODE

13. ABSTRACT (*Maximum 200 words*)

The FAST3D flow solver was used to determine the unsteady airwake and exhaust gas concentrations around the DDG-51 Flt-IIA superstructure and helicopter hangar areas. Previous simulations and analysis of the unsteady airwake show that the region over the helicopter landing deck has rapid, significant velocity fluctuations. A significant recirculated zone over the helicopter landing deck was seen which suggested the possibility of flow of stack gas into the helo hangars. Therefore, the flow field inside the hangars was investigated and compared against baseline results without the hangar doors open. The present results include analysis of 8 points inside the hangar areas and one point near the helicopter hover location. Analysis of the velocity fluctuations near the hover location showed that the fluctuations were in a range that would impact helicopter dynamics. Near and inside the hangars, the magnitude of the velocity was not significant; however, the gas concentrations in this region varied significantly due to the asymmetry of the superstructure. This report demonstrates that FAST3D can determine the asymmetric unsteady flow field based on a realistic representation of the ship superstructure, thus making it a useful tool for evaluating superstructure design options.

14. SUBJECT TERMS

Unsteady airwake simulations
Ship superstructure design
Complex geometry
Flux-Corrected Transport

15. NUMBER OF PAGES

19

16. PRICE CODE

17. SECURITY CLASSIFICATION OF REPORT	18. SECURITY CLASSIFICATION OF THIS PAGE	19. SECURITY CLASSIFICATION OF ABSTRACT	20. LIMITATION OF ABSTRACT
UNCLASSIFIED	UNCLASSIFIED	UNCLASSIFIED	UL

CONTENTS

DISCLAIMER NOTICE

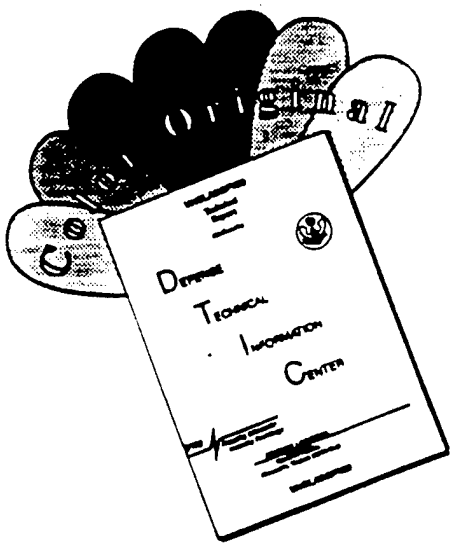

THIS DOCUMENT IS BEST QUALITY AVAILABLE. THE COPY FURNISHED TO DTIC CONTAINED A SIGNIFICANT NUMBER OF COLOR PAGES WHICH DO NOT REPRODUCE LEGIBLY ON BLACK AND WHITE MICROFICHE.

DDG-51 Flt-IIA Airwake Study
Part 2: Hangar Interior Flow

1. INTRODUCTION

The FAST3D flow solver was used to determine the unsteady airwake and exhaust gas trajectories and concentrations over highly complex ship superstructures using efficient, parallel algorithms. To date, other CFD calculations have used steady flow solvers over simplified ship configurations to determine average airwake velocity contours. The analysis of the unsteady flow simulations carried out for the DDG-51 Flt-IIA destroyer shows that the region over the helicopter landing deck has rapid, significant velocity fluctuations. Previous simulations showed a significant recirculated zone over the helicopter landing deck which suggested the possibility of flow of stack gas into the helo hangars. Therefore, the flow field inside the hangars was investigated and compared against baseline results without the hangar doors open. The present results include time histories of the velocity fluctuations and a frequency analysis. In addition, the unsteady airwake has been viewed with two-dimensional cross-sections of the stack gas distribution and velocity field contours.

2. BACKGROUND

Until recently it was perceived that it was not possible to compute the unsteady airwake about the detailed superstructure of an actual ship. Design evaluation and operability assessment in this field has therefore traditionally been based upon results from circulating water channel model-scale experiments and from extrapolation of previous full-scale experiments. This assessment is often carried out rather late in the design process. However, with high performance parallel computing becoming a mature, stable technology, problems which were previously limited either by CPU time or memory can now be solved. We have designed and implemented efficient, parallel algorithms to handle highly complex problems such as computing the unsteady airwake about a ship superstructure. Computations can now be made to aid in assessing the merits of a range of alternative configurations early in the design process, and, at a later stage, to plan experimental programs.

Another possible application of this computational method is to support the development of realistic flight simulators for at-sea landing conditions. Current flight simulators are, at best, based on steady-state calculations over simplified configurations to determine the ship airwake. A free air turbulence model, supposedly characteristic of atmospheric turbulence but lacking accurate spatial coherence, is sometimes superimposed on the steady ship airwake to generate an 'unsteady' airwake. The aircraft or helicopter is then flown through this synthetic flow. The flight simulator is fed the ambient flow values to determine the vehicle dynamics, but the flow field generated by the vehicle does not interact with the surrounding flow field. In other words, the downwash and airwake computations are completely decoupled.

Manuscript approved June 10, 1996

The downwash, particularly on approach and in a hover position, has been shown in our previous computations [1] to have a significant effect on the surrounding flow field.

3. COMPUTATIONAL METHODS

The unsteady airwake computations for the DDG-51 Flt-IIA destroyer have been described by Landsberg, *et al.* [2]. These computations used the unsteady flow solver, FAST3D, developed at the Laboratory for Computational Physics and Fluid Dynamics (LCP&FD). FAST3D has the capability of modeling highly complex configurations in an efficient manner. A parallel processing computer is well-suited for performing these computations due to the large computational grid and the large number of time steps required to acquire the unsteady data. The FAST3D code is based upon the Flux-Corrected Transport (FCT) algorithm [3,4,5] with the virtual cell embedding (VCE) method [6,7].

A necessary modification for ship airwake calculations is the addition of an atmospheric boundary layer model. In order to represent the atmospheric boundary layer over the open ocean, the model by Davenport [8] was incorporated into FAST3D. The atmospheric boundary layer is approximated by the power-law profile

$$u/u_{ref} = \left(z/z_{ref}\right)^n$$

where u_{ref} is a known velocity at a specified reference level z_{ref}. For the DDG-51 Flt-IIA simulations, the wind speed at the ship anemometer located on the mast is specified as 20 kts. The height at this location (z_{ref}) is 44.5 m. According to Davenport, the index n is usually found by matching the log- and power-law profiles at some appropriate elevation, yielding

$$n = 1/\ln\left(z_1/z_0\right)$$

Davenport gives the range of $0.01 > z_0 > 0.001$ for the roughness length scale in neutrally buoyant flow over the rough sea. A mean value of $z_0 = 0.005$ was chosen. An appropriate reference level (z_1) is the helicopter landing deck at a height of 10 m, which results in $n = 0.13$. This atmospheric boundary layer profile is imposed at the inflow. The implementation allows any wind angle to be specified relative to the ship heading.

4. RESULTS AND DISCUSSION

The goal in developing this model was to determine and assess potential hazards associated with the stack exhaust gases. Therefore, using FAST3D the unsteady flow field about the topside of the DDG-51 Flt-IIA destroyer was computed. Of special

interest was the helicopter landing area. In this particular region the velocity components and stack gas distribution were recorded. The unsteady data analysis consists of time histories of the velocity components and stack gas distribution, time-averaged velocity fluctuations, and power spectra of velocities at selected points of interest. To gain a better understanding of the global features of the airwake, two-dimensional slices of the flow quantities are presented.

4.1 DDG51 Problem Description

The computational representation of the DDG-51 Flt-IIA geometry (with the hangar doors closed) is shown in Figure 1. The superstructure contains several levels, each with sharp edges and drop offs causing vortex shedding over the landing deck. The exhaust gases from the engine stacks may recirculate down towards the landing deck causing both deck personnel hazards and landing approach hazards. In addition, the rear engine stack just forward of the landing deck may contribute to exhaust gas problems.

The computational grid for this problem is 192 x 64 x 48 (axial, vertical, transverse) which results in a grid resolution of one meter in each direction around the ship. Current efforts are directed toward tripling this resolution. Far from the ship, grid stretching is used to enlarge the domain. The ship speed for cases reported here is 20 kts into a 20 kt headwind, although any ship speed, wind speed or wind angle could be specified. The ambient temperature is specified as 100°F with an ambient density of 1.137 kg/m^3. There are two stack sizes, 8.5 ft. in diameter and 4 ft. in diameter. The larger stacks have (at the engine power level necessary to maintain a 20 knot speed into a 20 knot headwind) an exhaust temperature of 400°F and a density equal to 65% of the ambient density. The smaller stacks have a temperature of 325°F and a density equal to 73.6% of the ambient density. Buoyancy effects are included in the calculations via the density variations.

4.2 DDG51 Airwake Computations

The two cases to be compared are a baseline ship geometry (closed hangar doors) and the baseline ship with open hangar doors. Both cases were initialized with the atmospheric boundary layer profile and run out for 50 seconds of physical time. The flow is fully-developed by this point. Time histories are taken from 50 seconds to 75 seconds. The open hangar door cases were initialized similar to the closed hangar door cases except the hangar area was initialized with zero velocity. To illustrate the differences between closed hangar doors and open hangar doors, contour plots of the geometry and flow field are viewed with two-dimensional slices of the domain. Figure 2 shows contour plots of the stack gas distribution for the two cases. The top view and aft view show the structure of the hangar areas. The superstructure of the DDG-51 Flt-IIA is not symmetric which contributes to the flow field asymmetries. In this figure, values above 10% stack gas concentration are 'inside' the white cross-over line (red and yellow indicate a high concentration of stack gases). For this snapshot in time, the helicopter landing deck does not have stack gas concentrations

above this threshold. The values of the stack gas concentrations will be shown with time history plots. Figure 3 shows the contours of the velocity components above the helicopter landing deck and inside the hangar areas. These plots have transverse and vertical velocities with over 6 kt variations and recirculating flow throughout this region. There clearly is some flow into the hangar areas. These figures illustrate the global features of the flow. However, this analysis is inadequate for evaluating the stack gas concentration at the deck for personnel hazards or measuring the velocity fluctuations to determine the effect on an air vehicle.

To quantitatively analyze the flow field, 36 locations over landing deck region and 8 points inside the hangar areas were selected to record the gas concentration and unsteady velocities. These values were recorded every 0.005 seconds. The focus of this study is on the hangar interior flow; therefore, all eight points inside the hangar area will be analyzed while only one point near the hover location will be analyzed.

Previous calculations and analysis of the unsteady data showed that the helicopter landing region has rapid velocity fluctuations [1,2]. The velocity time history data were time-averaged over different periods to determine the longest interval for which significant fluctuations existed. Results with one-second time-averaging are compared with the instantaneous results. Finally, a frequency analysis of the data produces power spectral density plots to determine at what frequencies the energy is concentrated. This methodology helps in determining if the fluctuations will impact helicopter dynamics.

Analysis of the flow near the hover location will be presented first. For the baseline case with closed hangar doors, the time histories of the stack gas concentration and the three velocity components at a position of 21 ft. over the landing deck on centerline and 37 ft. aft of the hangar doors are shown in Figure 4. Each of these plots shows the unsteady nature of the flow field and the gusts that are experienced on and over the helicopter landing deck. Axial velocity has 25 kt gusts while both vertical and transverse velocity have 6 to 8 kt gusts. The peaks in gas concentration correlate with the gusts in the velocity components. The three prominent gas concentration peaks correspond to the time intervals during which the axial velocity is near its minimum. Conversely, a large axial velocity sweeps gases away from the helicopter landing deck. The time-averaged vertical velocity fluctuations and power spectral density are also shown in this figure. The vertical component of velocity was chosen since this component affects helicopter dynamics the most. With one-second averaging the vertical velocity varies from 0 kts to -2.5 kts. Most of the energy is concentrated in the 0.1 to 1.0 Hz range or 1 second to 10 second time domain. A helicopter will respond to frequencies in this range.

For the case with open hangar doors, similar data was collected at the hover location. Figure 5 shows the axial, vertical and transverse velocity at this location. At any given instant in time, the flow field can differ signficantly but the mean

values and RMS errors are quite close in value. Examination of the contours and point data at the hover location indicates that having the hangar doors open does not significantly influence the flow field over the landing deck.

The eight points inside the hangar have also been examined. Figure 6 shows two points (heights) 21 ft. inside the starboard hangar. The figures on the left correspond to a height 3 ft off the deck, while the figures on the right correspond to a height of 12 ft off the deck. At a height of 12 ft, the flow field inside the hangar is essentially transverse with a periodic increase in axial velocity towards the bow. The gas concentration is on the order of 2 to 2.5%. Depending on the contents of the gas, this may or may not be harmful to personnel. Close to the deck, transverse velocity fluctuates around 1 kt while at 12 ft above the deck, transverse velocity fluctuates around 3 kts. Figure 7 shows two points 21 ft. inside the port hangar at 3 ft and 12 ft. off of the deck. The components of velocity are very low, less than half a knot; however, gases are entering the port hangar as seen by the steady increase in the gas concentration. It should be noted that the gas concentrations inside the hangar were recorded at the same rate as the velocity components, the "staircase" nature of the profiles and apparent insensitivity of the interior hangar flow suggests the possibility of a long residence time for any gases drawn into the hangar. A comparison of Figures 6 and 7 show the effect on the flow field due to the asymmetry of the superstructure (see Figure 3). Figure 8 shows two points at the starboard hangar door at a height of 3 ft. and 12 ft. Similar to Figure 6 (21 ft. inside the starboard hangar), there is a periodic increase in axial velocity towards the bow, along with a noticable periodicity in the gas concentration. The asymmetry of the superstructure produces a more rapidly varying vortex on the starboard side of the landing deck. Figure 9 shows two points at the port hangar door. The gas concentrations at the port hangar door varies from 6 to 6.5%, a factor of two to three larger than the starboard side. The small rapidly varying vortex on the starboard side prevents gas build-up at and inside the starboard hangar area. The magnitude of the velocity near and inside the hangars was not significant; however, the gas concentrations near and inside the hangars varied significantly due to the asymmetry of the superstructure.

4.3 Calibration

To date neither model nor full-scale data for the DDG-51 Flt-IIA destroyer exists that can be used for code calibration purposes. We are currently pursuing avenues that would allow us to calibrate FAST3D for ship airwakes. However in the interim it is important to note that the algorithms used in FAST3D have been validated over many years with a number of different application problems such as subsonic free jets [9], mixing and near-field noise in jets [10], reactive flow in ram accelerators [11], and flows past simple geometries with known solutions [1,6].

5. SUMMARY AND CONCLUSIONS

A number of airwake simulations over the DDG-51 Flt-IIA destroyer have been

performed using the NRL code FAST3D. Analysis of these simulations showed that the region over the helicopter landing deck has rapid, significant velocity fluctuations. The frequency analysis shows that this unsteadiness is in a range that will affect helicopter dynamics. Analysis of the hangar area showed little effect on the flow field over the landing deck. The stack gas concentration inside the hangar areas was slightly over 2% while at the port hangar door, the gas concentrations were approximately 6%. Depending on the contents of the gas, this may or may not be harmful. This study was for a ship speed of 20 knots and a headwind of 20 knots. Other wind angles may have a more profound effect on the flow field inside the hangar areas, although most helicopter landings are performed with small angle variations from a straight headwind. This report shows that FAST3D can determine the asymmetric unsteady flow field based on a realistic representation of the ship superstructure. In conclusion, we believe FAST3D is a useful tool for evaluating superstructure design options.

Acknowledgments

This work was supported by the NAVSEA DDG51 Design Office (D. Ewing) with technical support from Steven Chun (SEA 03H32) and Michael Osborne (SEA 03X32).

6. REFERENCES

1. Landsberg, A.M., J.P. Boris., W.C. Sandberg, and T.R. Young, Jr., 1995, "Analysis of the Nonlinear Coupling of a Helicopter Downwash with an Unsteady Airwake", AIAA Paper 95-0047, American Institute of Aeronautics and Astronautics, Washington, DC.

2. Landsberg, A.M., J.P. Boris., W.C. Sandberg, and T.R. Young, Jr., 1993, "Naval Ship Superstructure Design: Complex Three-Dimensional Flows Using an Efficient Parallel Method", SCS Simulator Multiconference, San Diego, CA.

3. Boris, J.P. and D.L. Book, 1973. "Flux-Corrected Transport 1. SHASTA, A Fluid Transport Algorithm That Works." *J. Comput. Phys.* 11: 38-69.

4. Boris, J.P. and D.L. Book, 1976. "Solution of the Continuity Equation by the Method of Flux-Corrected Transport." Chapter 11 in *Methods in Computational Physics*, Academic Press, New York, 85-129.

5. Boris, J.P.; A.M. Landsberg; E.S. Oran; and J.H. Gardner, 1993. "LCPFCT - A Flux-Corrected Transport Algorithm for Solving Generalized Continuity Equations." NRL Memorandum Report 93-7192.

6. Landsberg, A.M.; J.P. Boris; T.R. Young, Jr.; and R.J. Scott, 1993. "Computing Complex Shocked Flows Through the Euler Equations." Proceedings of the 19th International Symposium on Shock Waves. Marseilles, France.

7. Young, Jr., T.R.; A.M. Landsberg; and J.P. Boris, 1993. "Implementation of the Full 3D FAST3D (FCT) Code Including Complex Geometry on the Intel iPSC/860 Parallel Computer." SCS Simulator Multiconference, San Diego, CA.

8. Davenport, A.G. 1982. *Engineering Meteorology*. E.J. Plate, Editor, Elsevier Scientific Publishing Company, Amsterdam, Netherlands, Chapter 12, 527-569.

9. Grinstein, F.F.; J.P. Boris; and O.M. Griffin, 1991. "Passive Pressure-Drag Control in a Plane Wake." *AIAA Journal* Vol. 19, No. 9, 1436-1442.

10. Kailasanath, K.; J.P. Boris; and A.M. Landsberg, 1993. "Effects of Shock Waves on Jet Mixing and Noise Generation." Proceedings of the 19th International Symposium on Shock Waves. Marseilles, France.

11. Li, C.; A.M. Landsberg; K. Kailasanath; E.S. Oran; and J.P. Boris, 1993. "Numerical Simulations of Reactive Flows in Ram Accelerators", Proceedings from the 29th JANNAF Combustion Meeting, Hampton, VA.

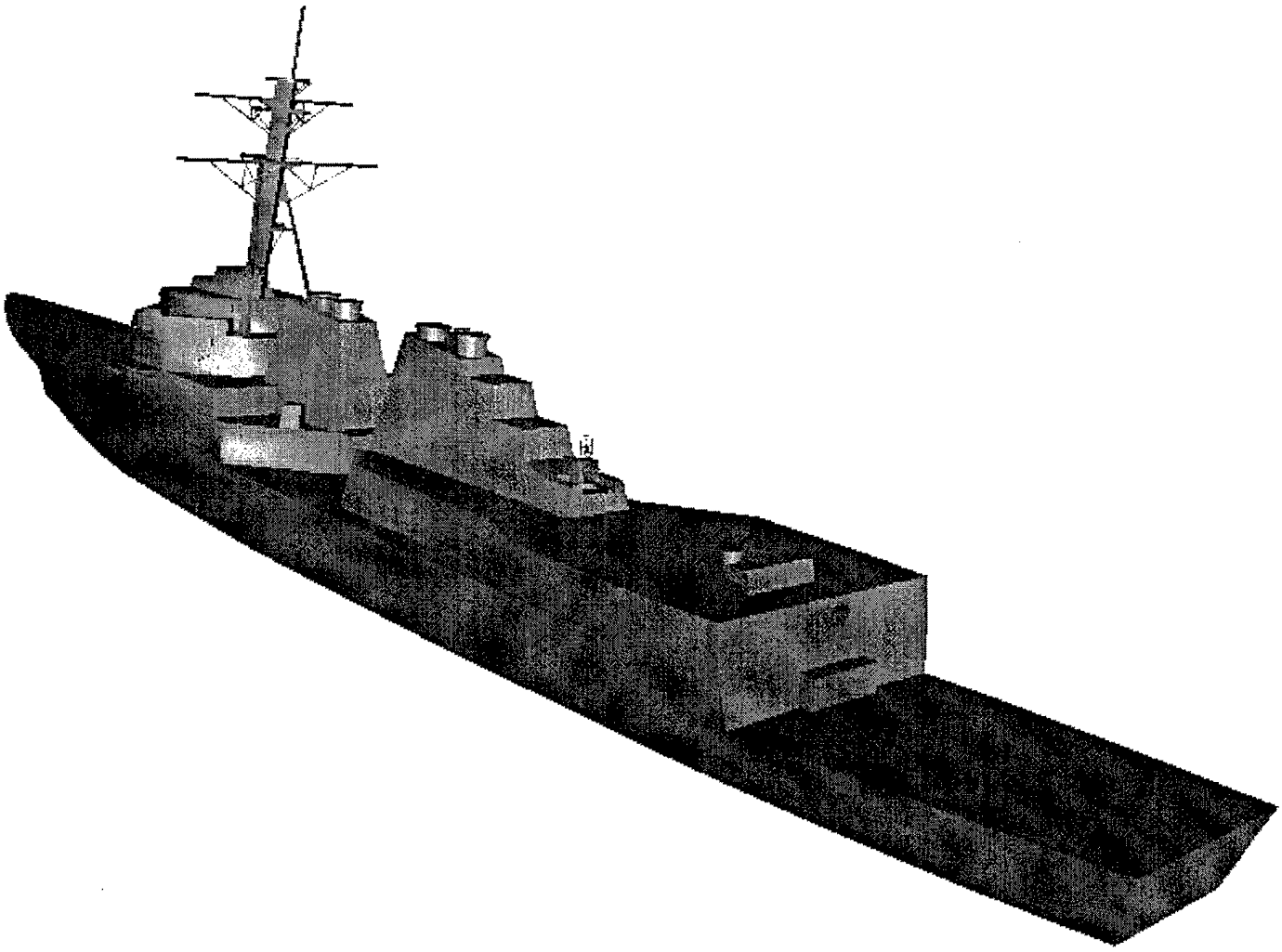

Figure 1. DDG-51 Flt.IIA geometry

STACK GAS CONCENTRATION

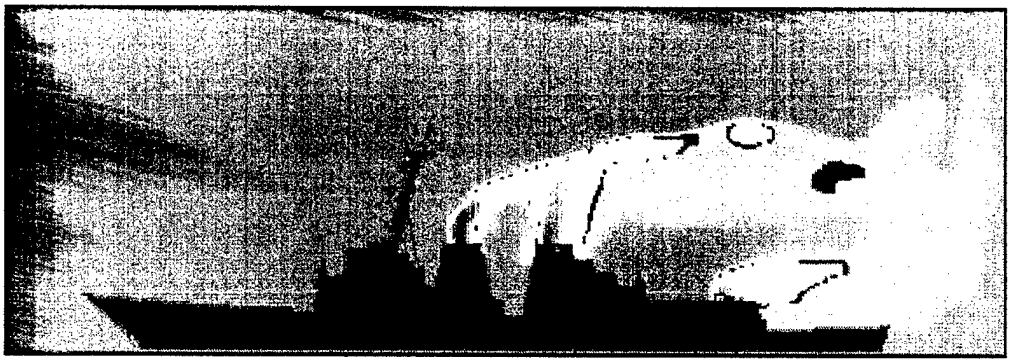

Centerline - Closed Hangar Doors

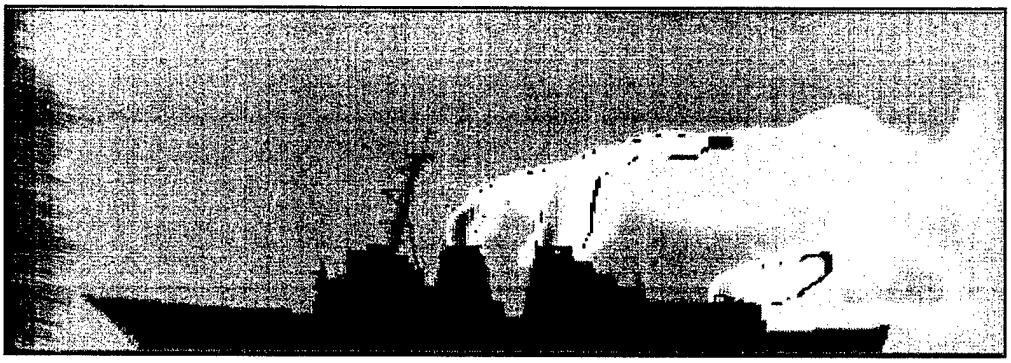

Centerline - Open Hangar Doors

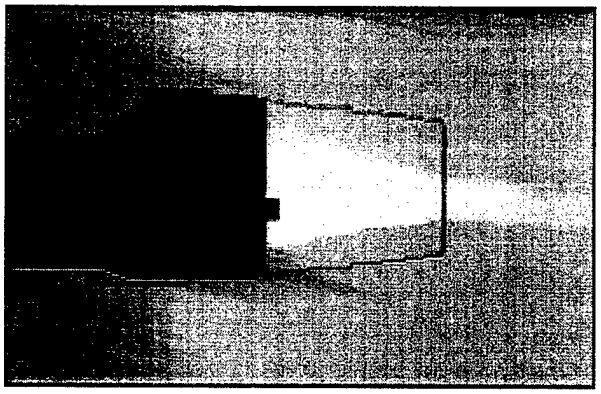

Top View - Closed Hangar Doors

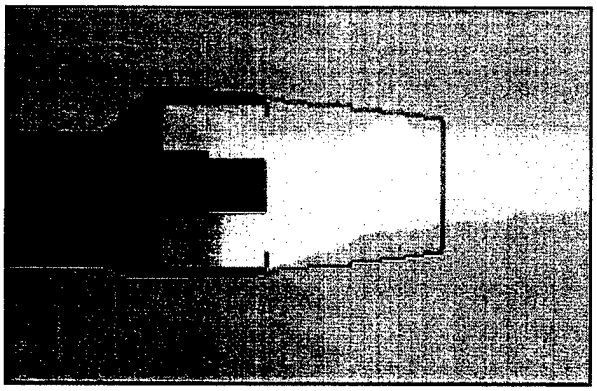

Top View - Open Hangar Doors

Aft View - Closed Hangar Doors

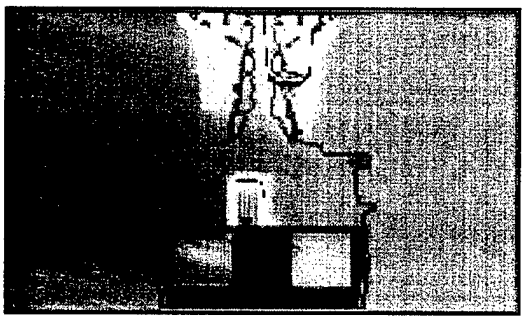

Aft View - Open Hangar Doors

Figure 2

VELOCITY CONTOURS

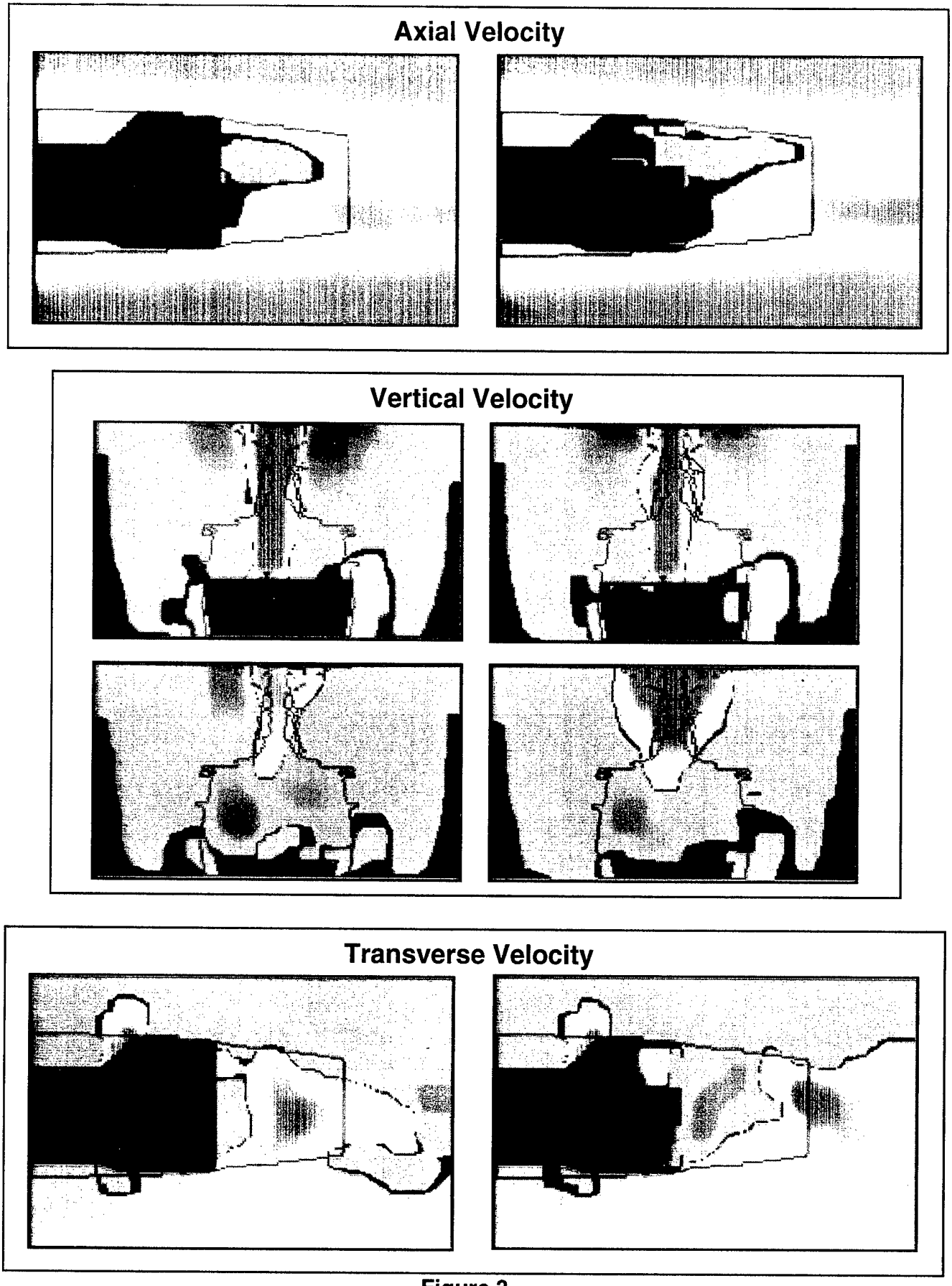

Figure 3

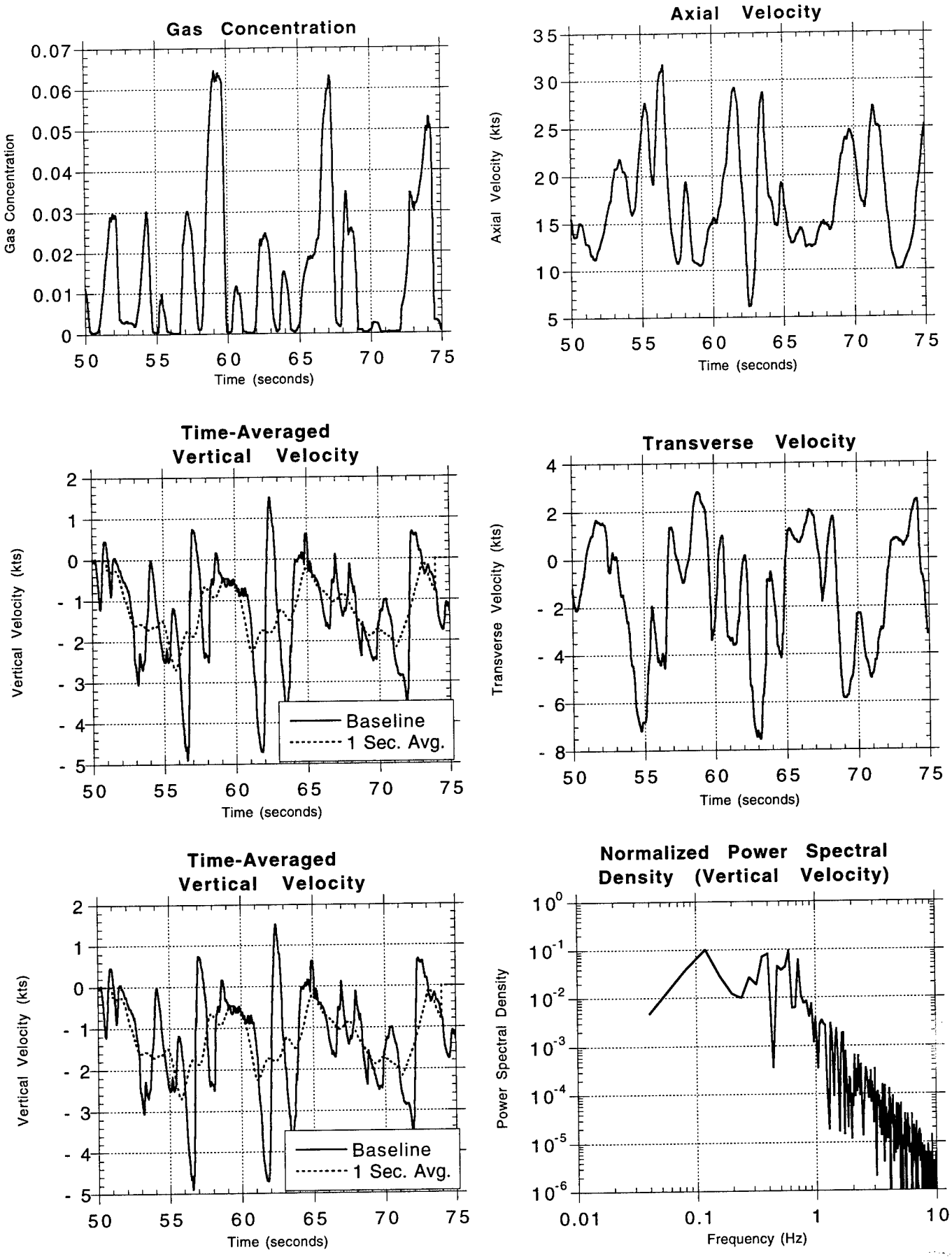

Figure 4. Hover Location - Closed Hangar Doors
21 ft. over landing deck, centerline, 37 ft. aft of hangar doors

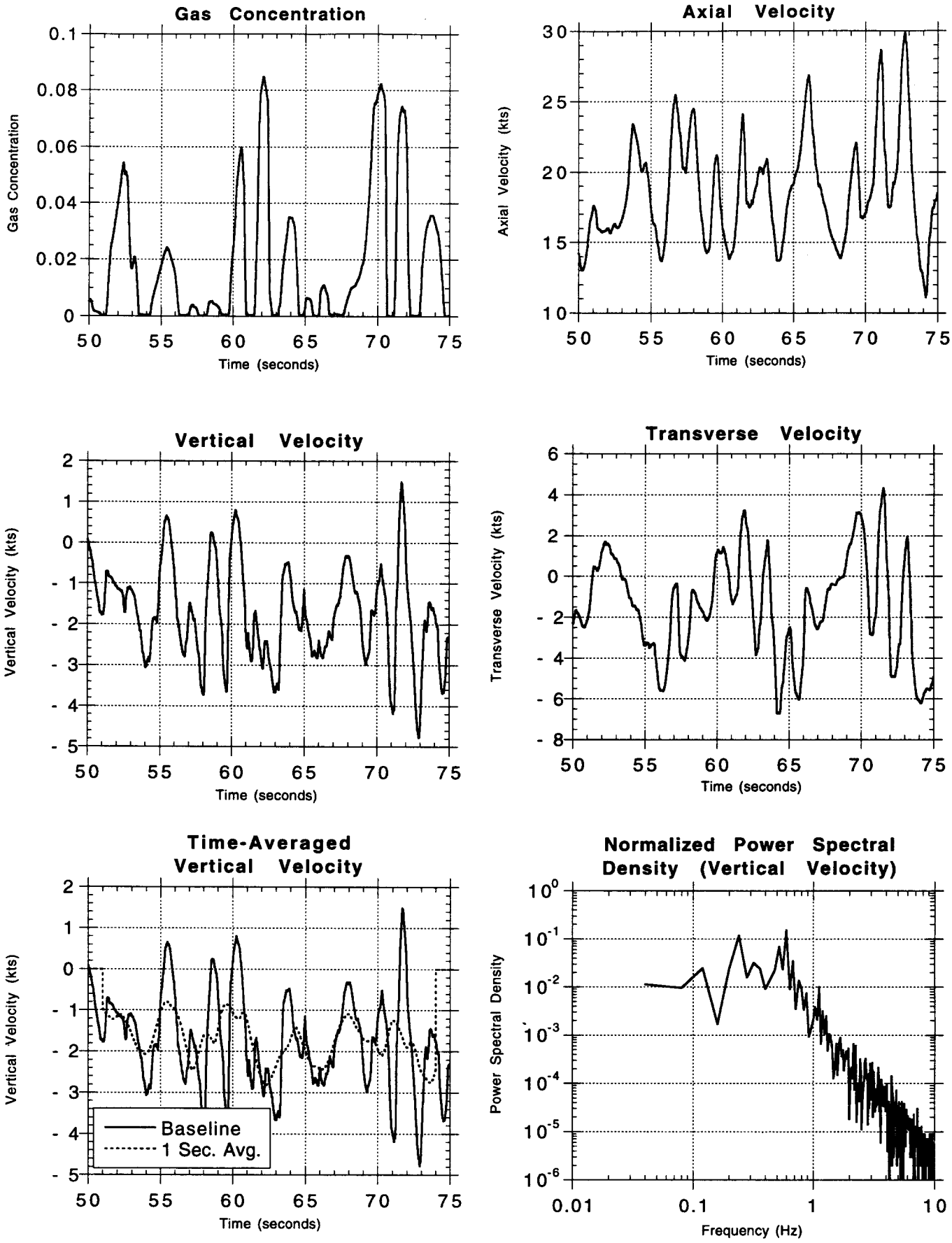

Figure 5. Hover Location - Open Hangar Doors
21 ft. over landing deck, centerline, 37 ft. aft of hangar doors

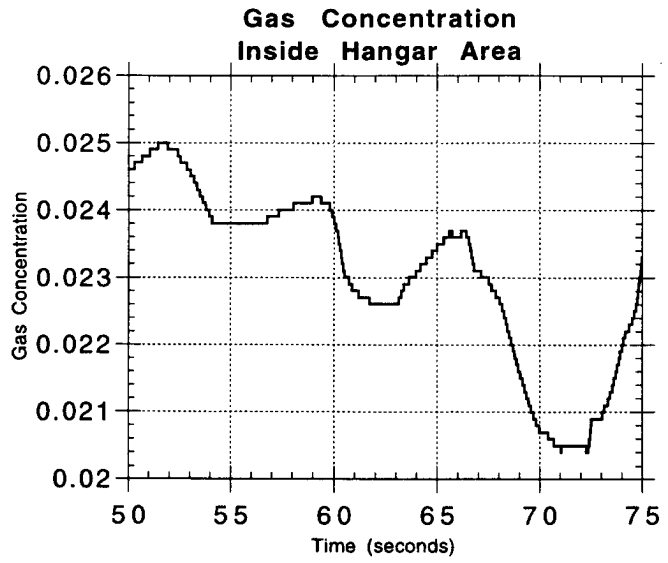

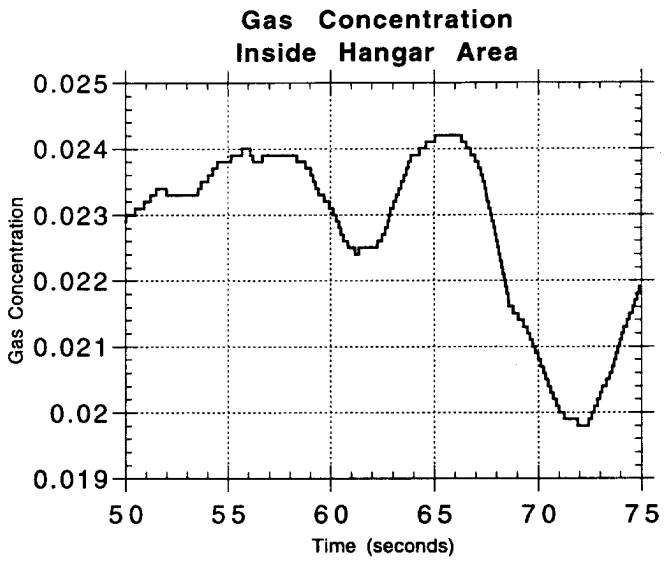

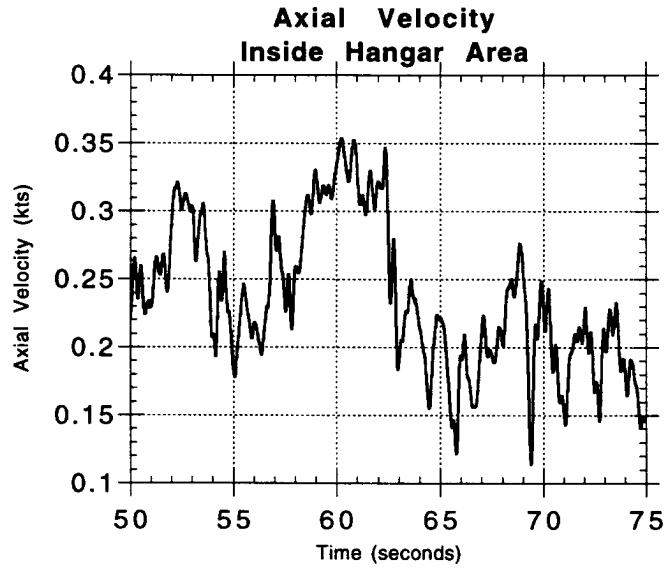

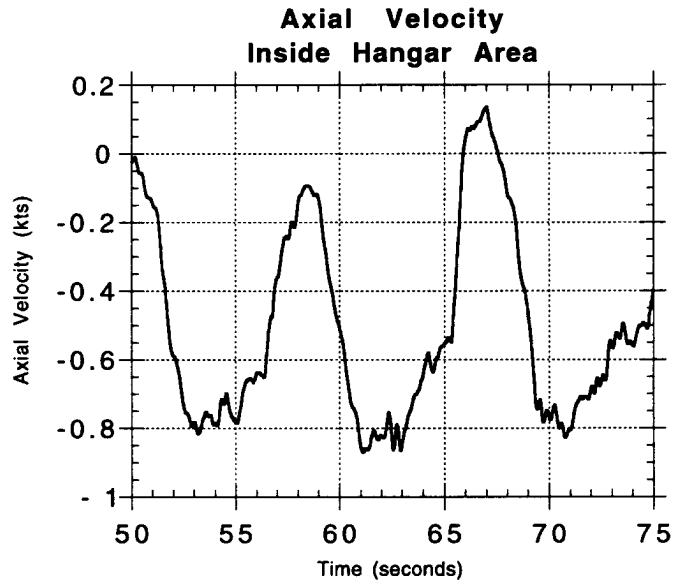

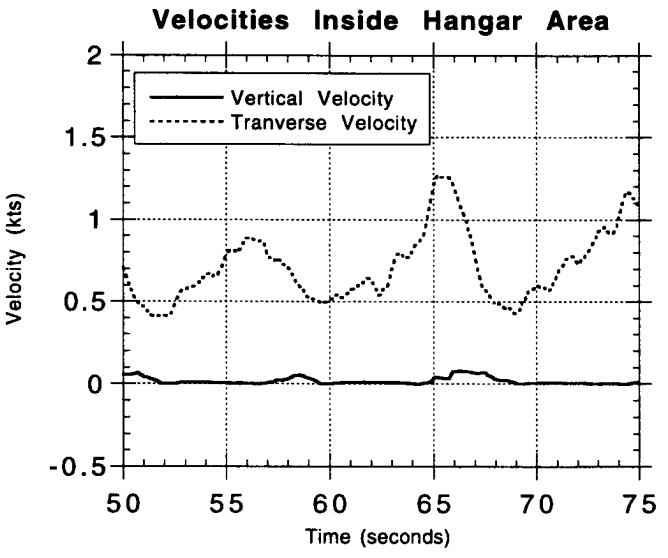

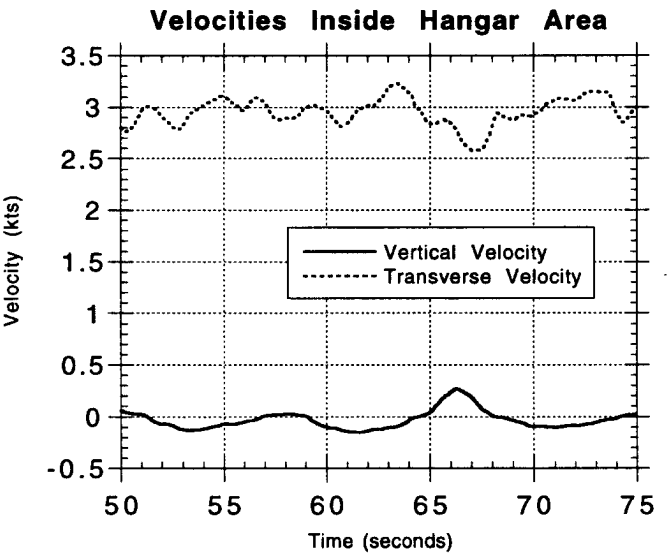

Figure 6.
21 ft. inside starboard hangar, centerline
Left - 3 ft. above deck
Right - 12 ft. above deck

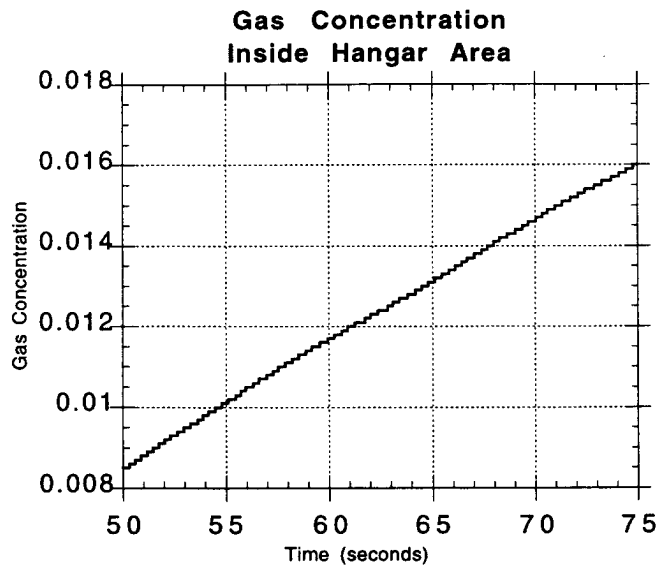

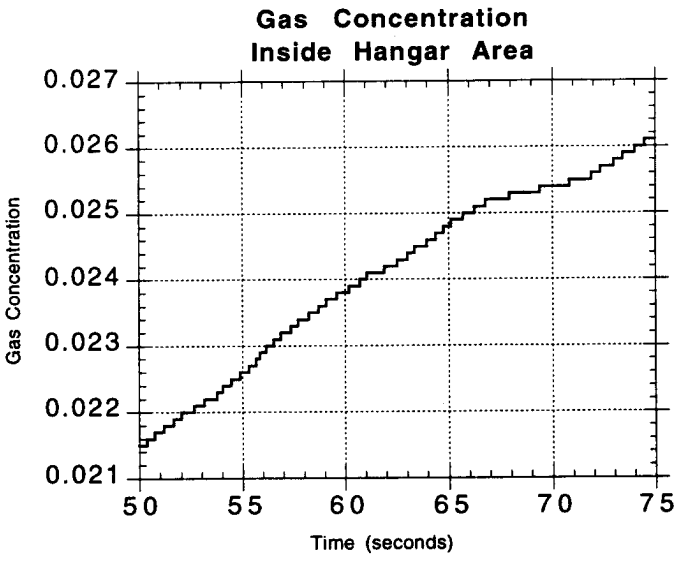

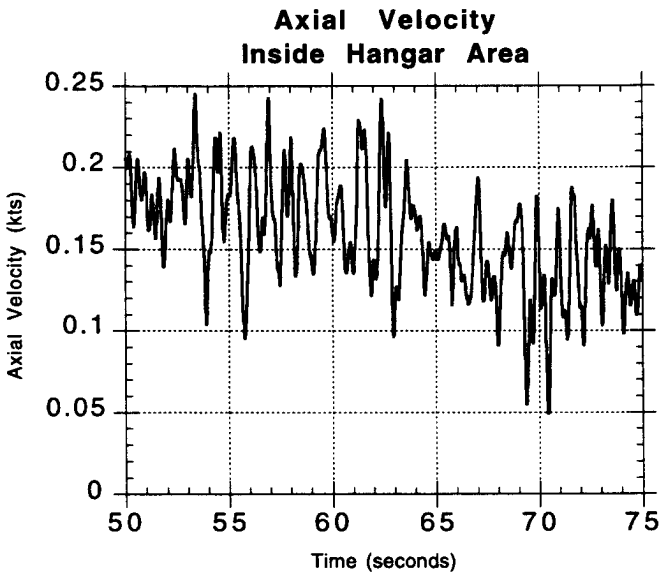

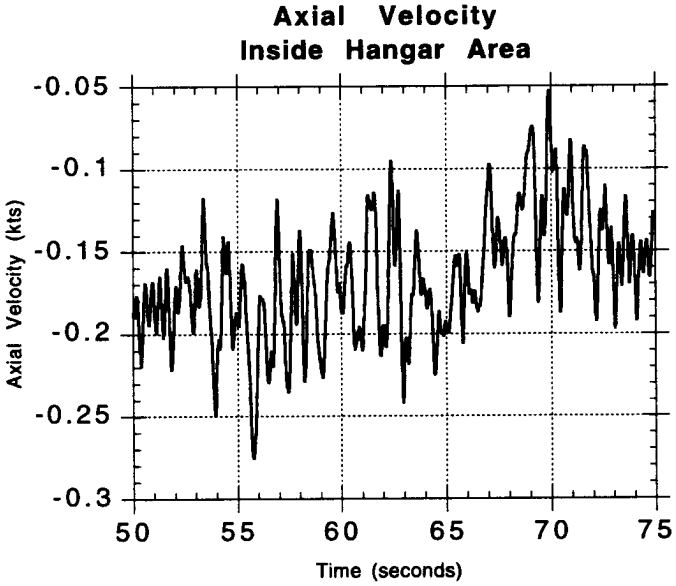

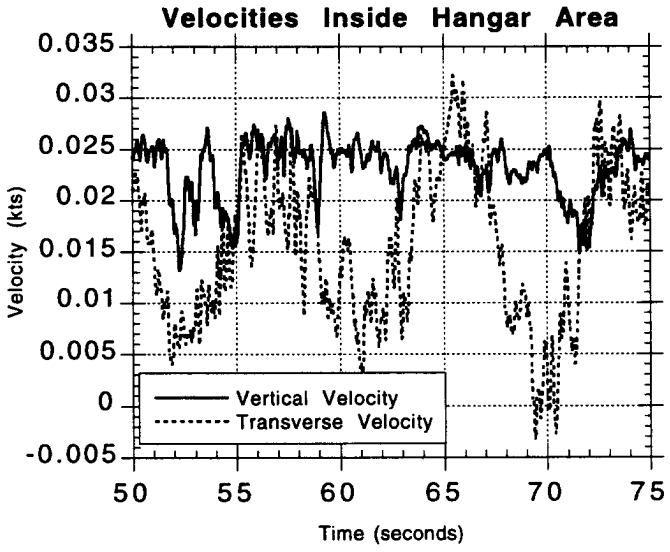

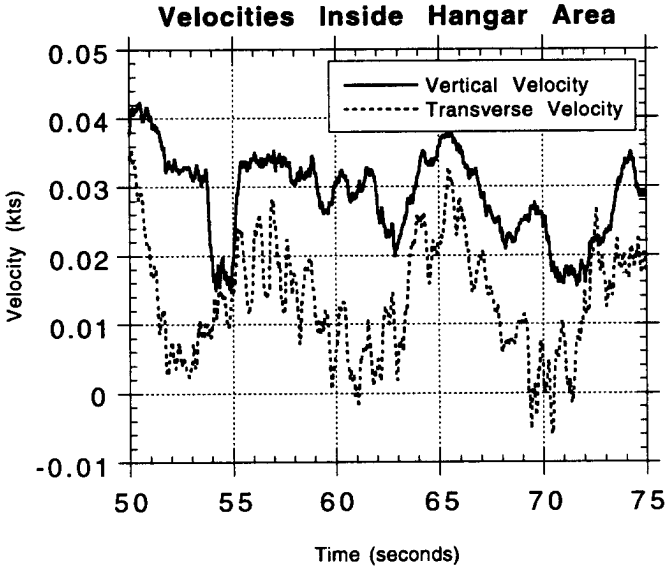

Figure 7.
21 ft. inside port hangar, centerline
Left - 3 ft. above deck
Right - 12 ft. above deck

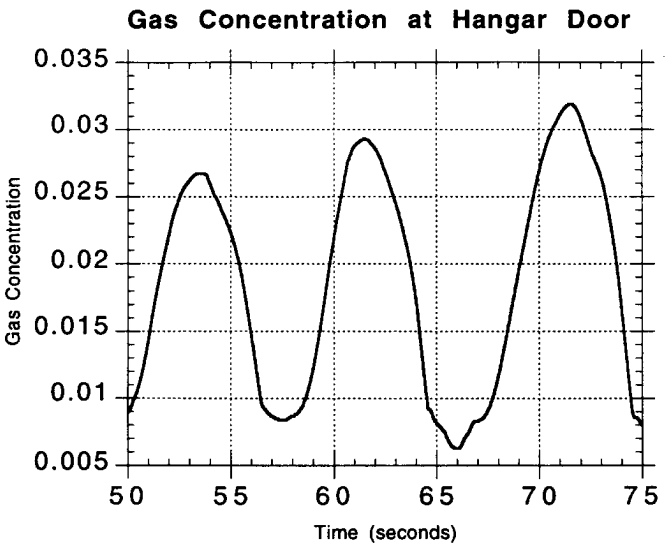

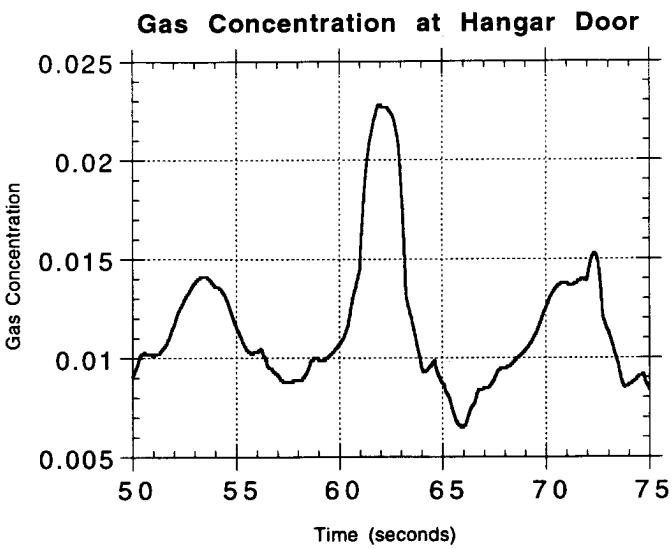

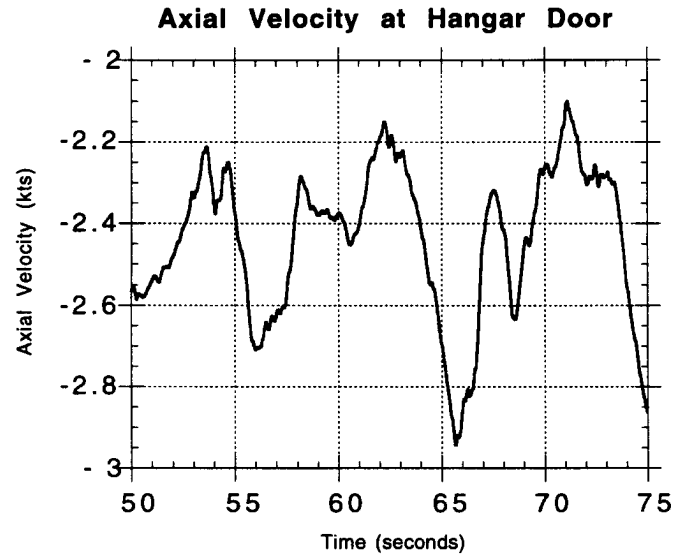

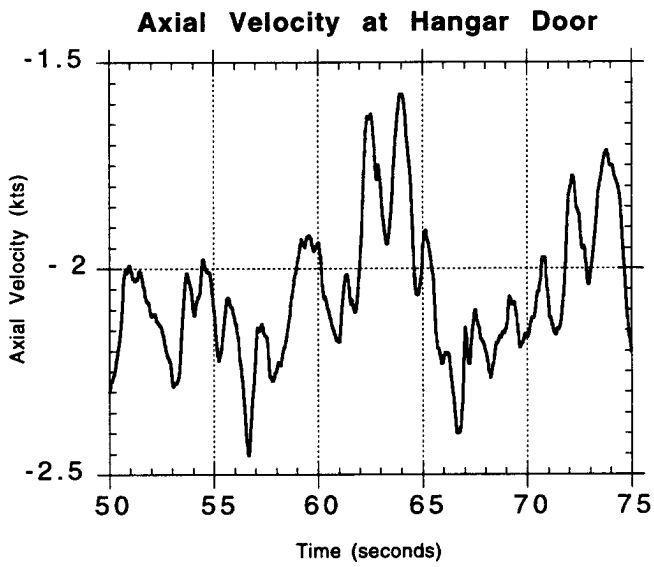

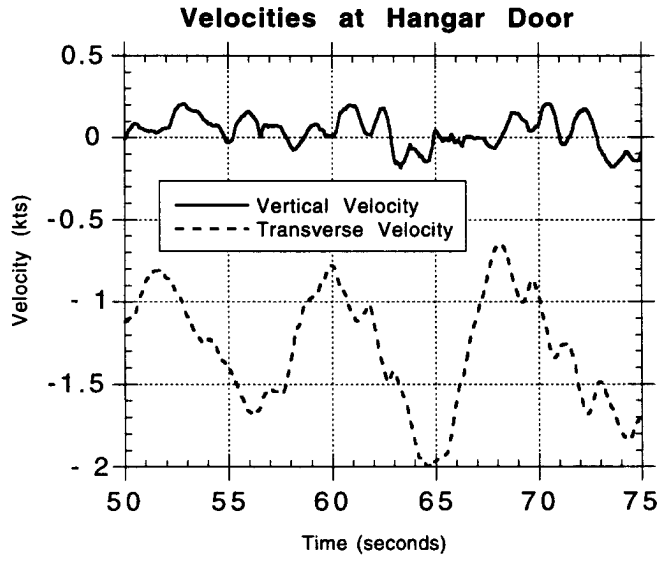

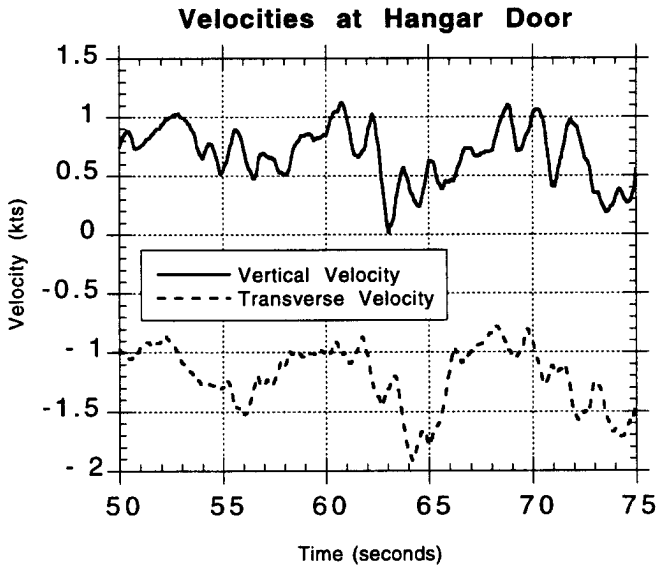

Figure 8.
At starboard hangar door, centerline
Left - 3 ft. above deck
Right - 12 ft. above deck

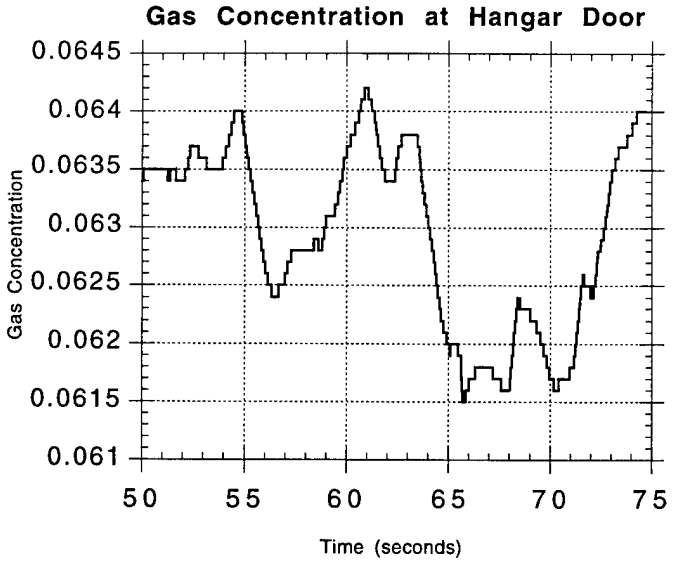

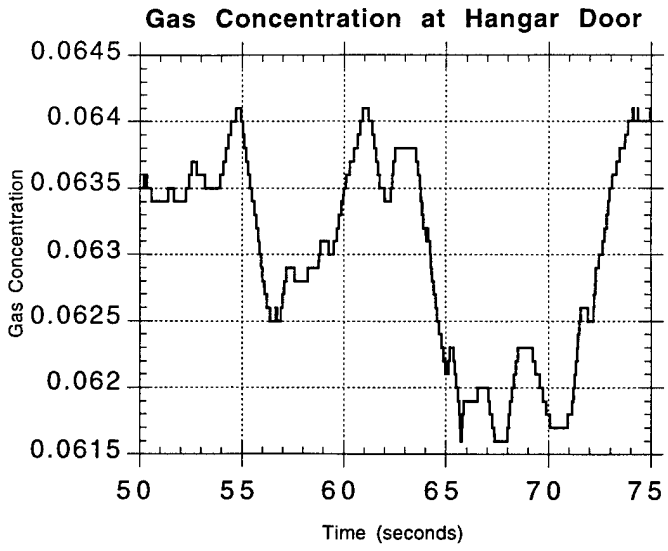

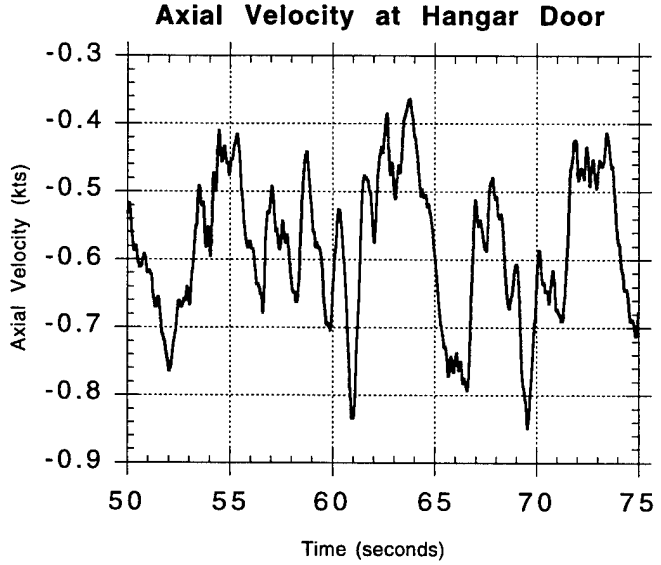

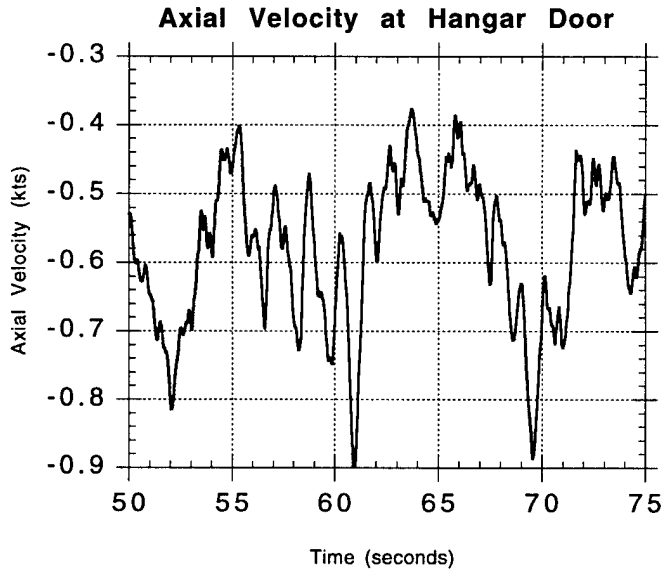

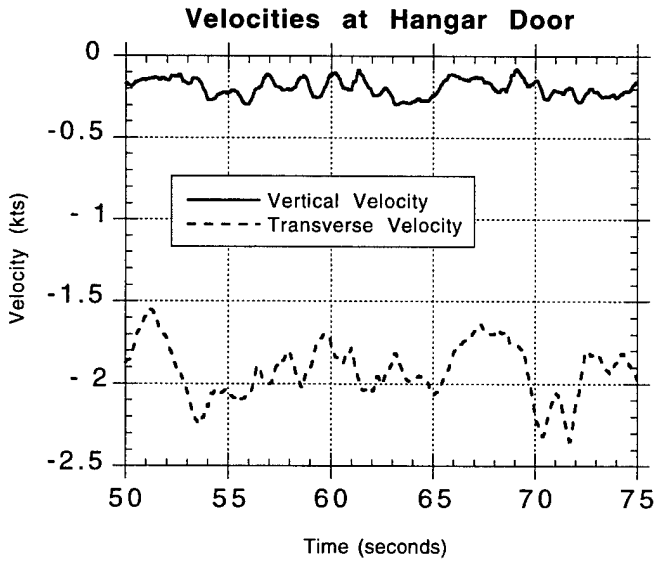

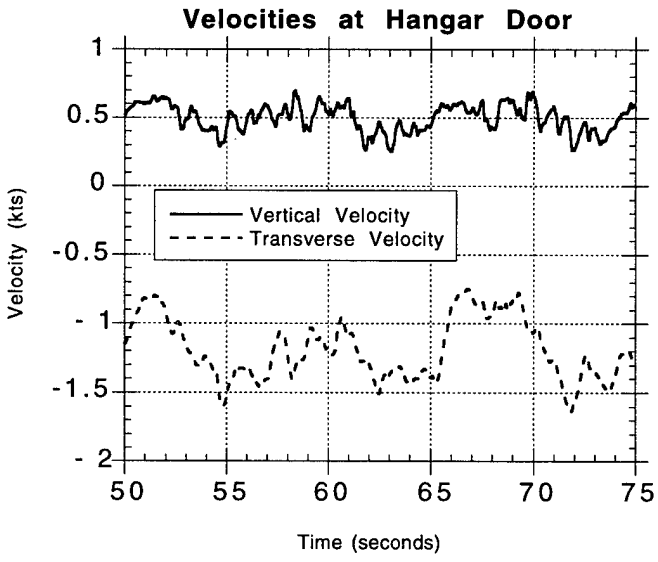

Figure 9.
At port hangar door, centerline
Left - 3 ft. above deck
Right - 12 ft. above deck